

# **Cryocooler Resonance Characterization**

R.G. Ross, Jr., D.L. Johnson, G.R. Men, and G. Smedley

Jet Propulsion Laboratory  
California Institute of Technology  
Pasadena, California 91109

## **ABSTRACT**

An important issue in the design and scaling-up of Stirling cryocoolers is achieving good drive motor efficiency and launch survivability. The important common thread linking these two topics is the dynamic resonant response of the compressor and displacer moving masses. The fundamental equations governing cryocooler mechanical efficiency and launch vibration response are presented and explored in terms of their implications for cooler design. The resonant frequency, damping, and drive motor force parameters associated with the cooler are shown to be key to efficient operation. Means of measuring these parameters are presented and shown to have broad applicability to additional parameters such as drive stiction and vibration transmitted to the instrument. The resonant parameters of the BAe 55K AIRS proof-of-concept cooler are used as an example to demonstrate the good correlation between the analytical fundamentals and the measured characteristics of a state-of-the-art cryocooler design.

## **INTRODUCTION**

The growing demand for long-wavelength infrared imaging instruments for space observational applications, together with the successful flight of the Oxford University ISAMS Stirling-cycle cooler, has led to the ongoing development of several second-generation Stirling-cycle cryocoolers that are scaled up in size from the original Oxford design. To ensure the success of these cooler developments, the Jet Propulsion Laboratory (JPL) has been carrying out an extensive cryocooler characterization program since 1989.<sup>1</sup> Following extensive characterization of the British Aerospace (BAe) 80K "Oxford" cooler<sup>2-6</sup>, more recently the JPL program has been expanded under Air Force and NASA sponsorship to focus on the larger capacity BAe 55K and 50-80K coolers<sup>7</sup>, and similar coolers from other manufacturers.<sup>8</sup>

An important topic with the new larger cooler designs is the subject of cooler drive motor efficiency and launch survivability. The important common link between these two topics is the dynamic resonant response of the compressor and displacer moving masses. The resonant frequency, damping, and drive motor force parameters associated with the cooler are key to efficient operation, and means of measuring these parameters have broad applicability to additional parameters such as drive stiction and vibration transmitted to the instrument.

This paper uses the BAe 55K cooler as an example to explore the important cooler drive resonance parameters, including the fundamental governing equations and useful measurement techniques.

## LINEAR COOLER DRIVE FUNDAMENTALS

Split Stirling coolers of the Oxford/BAe type are based on linear drive motors in both the compressor and displacer as shown in Fig. 1. In the Oxford cooler concept, the compressor piston and expander displacer are both suspended on flexure springs that allow precise linear motion in the axial drive direction, but minimize excursion in the radial piston-clearance direction. This provides long life by minimizing piston or displacer contact and wear during operation. In most linear drive coolers, the drive force is provided by a voice-coil driven permanent magnet motor similar to that used in a conventional audio speaker.

### Linear Drive Motor Relationships

In a linear voice coil drive motor, the applied force is proportional to the electrical current in the drive coil, the flux density of the magnetic field in the gap occupied by the coil, and the total length of coil wire that is in the magnetic field, i.e.<sup>9</sup>

$$F/i = BL \times 10^{-6} \quad (1)$$

where

- F = motor force (N)
- i = coil current (amps)
- B = magnetic flux density in the gap (lines/cm<sup>2</sup>)
- L = length of coil wire in the gap (cm)
- 10<sup>-6</sup> = conversion constant

In designing an efficient linear drive motor, consideration must be given to minimizing the i<sup>2</sup>R losses in the coil, and achieving a coil that is well matched to the cooler drive voltage. The back emf generated by the coil when it is moving in the magnet gap is the primary voltage-establishing parameter. Interestingly, the back emf for a given coil velocity is determined by the same physical parameters as govern the generated drive force, i.e.<sup>9</sup>

$$E/\dot{x} = BL \times 10^{-6} \quad (2)$$

where

- E = generated back-emf coil voltage (volts, o-p)
- x = coil velocity (meters/second, o-p)
- B = magnetic flux density in the gap (lines/cm<sup>2</sup>)
- L = length of coil wire in the gap (cm)
- 10<sup>-6</sup> = conversion constant

This back-emf motor constant can be easily measured by driving the cooler motor externally (e.g. pneumatically), and measuring the generated voltage for a given stroke; thus

$$E/\dot{x} = 450 E_{rms}/(f x_{p-p}) \quad (3)$$

Where

$E_{rms}$  = open-circuit back-emf voltage (volts, rms)

$f$  = drive frequency, Hz

$x_{p-p}$  = stroke amplitude, mm (p-p)

When the cooler is in operation, the required cooler drive voltage is the sum of the back-emf voltage and the  $iR$  drop in the drive coil due to the drive current ( $i$ ) and the coil impedance ( $Z \approx R$ ); i.e.

$$V = iR + E \quad (4)$$

Note that the terms in Eq. 4 are vectors, and scalar addition can only be used if both  $iR$  and  $E$  are in-phase. This in-phase condition turns out to be the maximum efficiency condition, and thus is a primary goal of the compressor drive suspension design.

### Drive Motor Efficiency

**Linear** motors consume power in three principal ways: 1) by doing useful work on the applied load, 2) by dissipating  $i^2R$  losses in the drive coil, and 3) by doing work to overcome various internal frictional forces impeding the motor motion. These frictional forces, caused by windage, mechanical friction, and eddy current forces, may become significant in a poor motor design. Because  $i^2R$  losses are generally the dominant loss term in a good motor, cooler motor efficiency has historically been expressed as<sup>10</sup>

$$\text{Motor efficiency} = (\text{input power} - i^2R)/(\text{input power}) \quad (5)$$

Because power is the integrated dot product of force and velocity, only the component of an applied force that is in-phase with the piston velocity consumes input power. Similarly, from Eqs. (1) and (2), only the current component in-phase with the back-emf does useful work. Currents 90° out of phase with the velocity can be thought of as capacitive or inductive circulating currents that only contribute to  $i^2R$  losses. A motor that operates efficiently thus has a near unity power factor, where power factor is defined as the cosine of the phase angle between the input drive voltage and the input drive current. The power factor is also the input power consumed divided by the product of the true rms voltage times the true rms current.

A key goal of cooler design is thus to minimize or eliminate drive currents or forces that are 90° out of phase with the drive velocity. Because the mechanical and gas spring forces restraining the piston movement, and the inertial forces required to accelerate the piston, are opposite in sign and 90° out of phase with velocity, minimizing the sum of these forces is key to high cooler efficiency. Since the inertial forces are dependent on the drive frequency and moving mass, and the stiffness forces are not, the sum of these 900-forces can be manipulated and nulled by appropriately selecting the drive frequency and the moving mass. This condition of equal and opposite spring and inertia forces is known as the resonant condition for a spring-mass system,

and occurs at a single drive frequency known as the natural frequency. Achieving resonance at the cooler drive frequency is thus important to high cooler motor efficiency.

### Cooler Drive Resonance Parameters

The primary determiners of the compressor resonant frequency are the moving mass of the compressor (M) and the total elastic spring constant (K) of the combined compressed gas and suspension springs. Since the gas and suspension springs act in parallel, the total elastic spring constant (K) is given by

$$K = (1/K_s + 1/K_g)^{-1} \quad (6)$$

where

$K_s$  = Spring constant of suspension springs (N/m)

$K_g$  = Spring constant of the compressed gas (N/m)

Generally the gas spring of the compressor is modestly stiff compared to the suspension springs, and thus the gas spring contributes the majority of the total stiffness. Because the spring constant of the gas is roughly proportional to the fill pressure, inversely proportional to the working gas volume, and proportional to the 4<sup>th</sup> power of the piston diameter, the spring constant of the compressor is very sensitive to its size and geometry. In contrast, the gas spring of the displacer is generally relatively weak compared to the stiffness of the suspension springs, and thus the stiffness of the displacer is principally determined by the suspension spring stiffness. The displacer stiffness is therefore much less sensitive to scaling of the cooler's size.

These mechanical elements of a linear-drive, Stirling-cycle cooler combine to closely approximate a classic single-degree-of-freedom spring-mass system as schematically illustrated in Fig. 2. This system has a natural frequency ( $f_o$ ) defined by

$$f_o = 1/2\pi [K/M]^{1/2} \quad (7)$$

where

$f_o$  = natural frequency (Hz)

$K$  = spring stiffness (N/m)

$M$  = moving mass (kg)

Because of the work performed on the gas internal to the cooler, the resonant piston and displacer systems also include relatively large velocity-dependent forces, denoted by the damper (C) in Fig. 2. The degree of damping is described by the ratio ( $\zeta$ ) of the damping coefficient (C) to critical damping coefficient (CC). The critical damping coefficient CC is defined as

$$CC = 2 (KM)^{1/2} = 4\pi M f_o \quad (8)$$

where

CC = critical damping coefficient (N-sec/meter)

Because the damper force ( $F_c = C \times \text{velocity}$ ) is in-phase with the velocity, it is the only power dissipating force in a dynamic system. The level of power dissipation is given by

$$P_c = \frac{1}{2} C \dot{x}^2 = 4.935 \times 10^{-6} f^2 x_{p-p}^2 \zeta C_c \quad (9)$$

where

PC = power dissipation, watts

$\dot{x}$  = piston/displacer velocity (o-p), m/s

f = drive frequency, Hz

$x_{p-p}$  = peak-to-peak displacement amplitude, mm

C = damping coefficient, N-s/m

$\zeta$  = damping ratio (C/CC)

CC = critical damping coefficient, N-s/m

### Response to Sinusoidal Forced Excitation

The classic solution for the amplitude response of the moving mass to a sinusoids' drive force ( $F_d \sin 2\pi ft$ ) is given by<sup>11</sup>

$$x/x_o = 1/\{[1 - (f/f_o)^2]^2 + [2\zeta(f/f_o)]^2\}^{1/2} \quad (10)$$

where

x = piston/displacer motion amplitude (o-p)

$x_o$  = zero frequency amplitude =  $F_d / K$

f = drive frequency, Hz

Eq. (10) is plotted in Fig. 3 in terms of the damping ratio ( $\zeta = C/C_c$ ) and the frequency ratio (f/f<sub>o</sub>). When a modest degree of damping is present, the maximum response amplitude and amplitude gain are seen to occur at a frequency that is somewhat less than the natural frequency. This frequency of maximum response is referred to as the resonant frequency (f<sub>R</sub>). The amplitude gain (Q<sub>o</sub>) at the natural frequency is directly related to the damping ratio ( $\zeta$ ) by

$$Q_o = C_c/2C = (2\zeta)^{-1} \quad (11)$$

Another situation of interest to the cryocooler integrator is the vibration force transmitted to the host instrument from the cooler's moving mass. If the cooler mount is very rigid (i.e. the mount resonance is well above the cooler drive frequency) then the force transmission ratio is given by<sup>11</sup>

$$F_t/F_d = (f/f_o)^2 / \{[1 - (f/f_o)^2]^2 + [2\zeta(f/f_o)]^2\}^{1/2} \quad (12)$$

where

F<sub>t</sub> = vibration force amplitude (o-p) transmitted to the cooler mount

F<sub>d</sub> = force amplitude (o-p) from cooler motor drive coil

Eq. (12) is plotted in Fig. 4. Note from Figs. 3 and 4 that high frequency drive forces caused by nonlinearities and current harmonics above the drive frequency are directly transmitted to the support structure and cause little piston motion. This relationship will be used later to measure the drive motor force/current transfer function as defined in Eq. (1). Note also that they are 90° out of phase with the piston velocity; thus they do no work, but contribute directly to I<sup>2</sup>R losses.

## CHARACTERIZATION OF BAe COOLER RESONANCE PARAMETERS

Although the analytical understanding of the cooler drive parameters--as articulated in the above equations--is reasonably well developed, obtaining the actual parameter values generally requires empirical measurements. This is because many of the cooler parameters such as the spring constant of the compressed gas, the flux density in the voice coil drive, and the velocity dependent work in the compressor and displacer are only roughly predictable.

To measure the compressor and displacer resonance parameters, the BAe 55K cooler was mounted on JPL's force dynamometer; this allows the compressor and displacer transmitted interface forces ( $F_i$ ), as well as the piston and displacer strokes, to be quantified. The actual test involves conducting a constant-amplitude, sinusoidal-current frequency sweep through the region of the cooler's resonant frequency. Because of the relationship between current and drive force as described by Eq. (1), the test closely approximates a constant sinusoidal force input over the range of drive frequencies. Compressor and displacer motion amplitude and phase relative to the drive current are measured using the cooler's built-in position sensing (LVDT) transducers,

Plots of the measured piston/displacer resonant response closely approximate the vibration frequency response and force transmissibility curves presented in Figs. 3 and 4. The cooler's parameter values are quantified by least-squares fitting the response equations (Eqs. (10) and (12)) to the measured curves. Table 1 summarizes the measured resonance and drive parameters for the BAe 55K AIRS cooler at both ambient and cryogenic temperatures. The ambient-temperature data are those applicable during launch and cooler start-up, while the cryogenic data are applicable for normal operation when the cold-tip is at cryogenic temperatures. Note that the measurement technique provides for complete characterization of the cooler including such parameters as the motor force constant, the moving mass, the spring stiffness, and the damping. Details of the measurements are described below.

### Compressor Drive Resonance Characteristics

As seen in Table 1, the resonance characteristics of the compressor change somewhat between ambient and cryogenic temperatures. This is because the stiffness of the gas spring drops with decreasing gas pressure as gas density increases in the cold-finger. Note that the damping also increases somewhat at cryogenic temperatures. This damping at cryogenic temperatures is a measure of the losses in the refrigerator when the displacer is not operating; these losses can be computed using Eq. (9). In contrast, the ambient damping is important in determining the extent of piston attenuation during launch, and will be revisited later when discussing launch behavior.

Figures 5 and 6 display example frequency response data for both the compressor stroke and transmitted force at three different drive-current levels. Note that the damping also increases somewhat with increasing stroke; this is typical of most structural systems. The natural frequency at cryogenic temperatures is found to be desirably close to the 48.5 Hz drive frequency and leads to measured power factors around 0.98. The measured drive motor efficiency of the compressor is presented in Fig. 7, and can be seen to closely match the

measured resonant response. The maximum efficiency of around 74% is typical for motors of this type.

### Displacer Drive Resonant Characteristics

As seen in Table 1, the primary feature of the displacer that changes between ambient and cryogenic temperatures is the damping. This is no doubt linked to the increased density of the gas in the cold-finger at cryogenic temperatures. Because the damping force is in-phase with the displacer velocity, this high degree of damping represents an important power loss term in the displacer. Using Eq. (9) this power dissipation is computed to be approximately 0.45 watts for a nominal displacer stroke of 3 mm p-p and with the compressor stroke restrained to zero. Figures 8 and 9 display example frequency response data for both the displacer stroke and transmitted force at three different drive-current levels.

## RESONANCE EFFECTS ON LAUNCH VIBRATION RESPONSE

In addition to being important to cooler electrical efficiency, motor resonance characteristics are also key to the amplitude of piston and displacer motions excited during launch. The key issue is whether the excited motions during launch will cause the cooler piston and/or displacer assembly to hit their end stops and possibly damage the internal parts or knock the cooler out of alignment. The fundamental equation describing the amplitude of vibration for a given launch acceleration level ( $x$ ) is the same as Eq. (10) except that the input force is the negative product of the moving mass and the launch acceleration; i.e.  $F_d = -Mx$ . Thus

$$x/x_o = 1/\{[1 - (f/f_o)^2]^2 + [2 \zeta (f/f_o)]^2\}^{1/2} \quad (13)$$

where

- $x$  = piston/displacer motion amplitude (o-p), meters
- $x_o$  = zero frequency amplitude =  $M x / K = x / (2\pi f_o)^2$
- $\ddot{x}$  = launch acceleration amplitude (o-p),  $m/s^2$   
=  $9.81x$  (launch acceleration in  $g$ 's, o-p)
- $f$  = launch acceleration frequency, Hz
- $f_o$  = piston/displacer natural frequency, Hz

Note that  $X$  reduces to  $x / (2\pi f_o)^2$ , which is the displacement amplitude of the base excitation motion at the natural frequency of the cooler. Thus, the higher the natural frequency, the lower will be the resulting piston/displacer motion during launch for a given launch acceleration level. Because of the similarity between Eqs. (10) and (13), Fig. 3 is also a plot of Eq. (13).

From Fig. 3 it is clear that another means of controlling piston/displacer motion is to increase the damping, and thereby to reduce the gain ( $Q_o$ ) at the compressor and displacer natural frequencies. Figure 10 summarizes the computed piston/displacer motion amplitude (p-p) for a 15-g (o-p) sinusoidal launch acceleration and for various piston/displacer natural frequency and gain ( $Q_o$ ) levels. The 15-g level is a typical launch acceleration requirement for small spacecraft

devices with resonant frequencies below 100 Hz<sup>12,13</sup>. Note that the limited travel of the displacer makes it the more difficult element to protect against over-stroking during launch.

### Effects of Shorting the Drive Coils

One means of greatly increasing the damping during launch without imposing an efficiency penalty on the operating cooler is to electrically short the compressor and displacer drive coils. When the coils are shorted, the back emf voltage developed by each coil (Eq. (2)) generates a current proportional to the coil velocity and limited by the coil circuit resistance. This current develops a damping force ( $F_c$ ) opposing the coil motion as described by Eq. (1). '1'bus,

$$\begin{aligned} F_c &= [(force/amp) \times (volts/velocity) / resistance] \times (coil velocity) \\ &= C_c \dot{x} \end{aligned} \quad (14)$$

where

$$\begin{aligned} F_c &= \text{electrical damping force, N} \\ C_c &= \text{electrical damping coefficient, N-s/m} \\ \dot{x} &= \text{coil velocity, m/s} \end{aligned}$$

The components of the electrical damping coefficient are available from Eqs. (1), (2) and (3); thus

$$\begin{aligned} CC &= (BL \times 10^{-6})^2 / R \\ &= (Newtons/amp)^2 / R \\ &= (E/\dot{x})^2 / R \end{aligned} \quad (15)$$

where

$$\begin{aligned} B &= \text{magnetic flux density in the gap (lines/cm}^2\text{)} \\ L &= \text{length of coil wire in the gap (cm)} \\ R &= \text{total coil resistance including external wiring, ohms} \\ E/\dot{x} &= \text{back-emf/velocity from Eq. (3)} \end{aligned}$$

Note that  $BL \times 10^{-6}$  is the motor force constant (N/amp), which is easily measured and is reported in Table 1 for the BAe 55K cooler. Using this cooler as an example, the electrical damping coefficient obtained by shorting the O. 88-ohm compressor coil is given by

$$CC = (12.7 \text{ N/amp})^2 / 0.88 \text{ ohm} = 183 \text{ N-s/m}$$

When combined with the existing damping ( $\zeta = 0.17$ ) in the compressor, this gives a damping ratio of

$$\zeta_{total} = \zeta + C_c / C_c = 0.17 + 183/157 = 1.34 \quad (16)$$

where

$$cc = 157 \text{ N-s/m (from Table 1)}$$

## **Launch Vibration Testing of BAe 55K Cooler**

To measure the compressor and displacer response to launch excitation and validate the computations for the effect of motor shorting, the BAe 55K cooler was rigidly mounted to a large launch vibration test shaker as shown in Fig. 11. The cooler was then subjected to low frequency sinusoidal acceleration frequency sweeps from 15 Hz to 100 Hz at a constant level of 3 g (o-p) parallel to the cooler drive axis. During the 2 octave/minute sweeps, the cooler piston and displacer motions were recorded using the cooler's internal (LVDT) position transducers. The resulting piston/displacer amplitude-versus-frequency plots are presented in Figs. 12 and 13 for a variety of coil-shorting resistances ranging from open-circuit to short-circuit. Note that the frequency response curves closely resemble those in Figs. 5 and 8 for the electrically driven cooler. Similarly, Table 2 presents the good agreement between the response parameters measured in the 3-g sine test and those calculated using Eqs. (3, 8, 11, 13, 15, and 16) together with the measured cooler parameters in Table 1. The data also agree quite well with measurements made by BAe on their 80K cooler.<sup>13</sup>

## **DRIVE RESONANCE MEASUREMENT OF STICTION**

Another challenge facing the designers of mechanical coolers is the unwritten rule that a long-life cryocooler must avoid rubbing surfaces. The flexure bearings and piston clearance seals incorporated into the BAe 55K Stirling-cooler design are examples of the application of this rule. In trade for the exclusion of rubbing surfaces, linear Stirling coolers of this type face the challenge of maintaining tight manufacturing and assembly tolerances and high degrees of cooler dimensional stability over the cooler operating temperature range.

### **low Frequency Stiction Testing**

One means of verifying the absence of rubbing or contact is the low frequency stiction test. This test technique involves driving the cooler at extremely low frequencies (0.001 to 1 Hz) and plotting the required drive current -- which is proportional to drive force -- versus piston displacement.<sup>2</sup> At these low frequencies, gas pressure is extremely sensitive to piston clearance, and rubbing is made visible as stiction or discontinuity in the current-displacement plot. This test is useful under a wide variety of post-build environmental conditions and can be applied over the complete operating temperature range of the cooler.

### **High Frequency Stiction Testing**

An alternative method for measuring the presence of stiction is to introduce low level sinusoidal currents at the cooler's natural frequency and gradually increase the level until the threshold current for stiction breakaway is determined. To determine the variation in stiction along the stroke, the measurements are made using various dc piston/displacer off-sets. An advantage of this procedure over the low-frequency stiction test is that the threshold currents, and thus forces, can be very accurately measured; this is because the stiction-measuring current is ac, while the positioning current is dc.

## SUMMARY CONCLUSIONS

The important common thread linking the achieving of good drive motor efficiency and launch survivability is the dynamic resonant response of the compressor and displacer moving masses. The fundamental equations governing cryocooler mechanical efficiency and launch vibration response have been presented and explored in terms of their implications for cooler design. The resonant frequency, damping, and drive motor force parameters associated with the cooler are shown to be key to efficient operation. Means of measuring these parameters are presented and are shown to have broad applicability to additional parameters such as drive stiction and vibration transmitted to the instrument. The resonant parameters of the BAe 55K cooler have been presented and used to demonstrate the good correlation between the analytical fundamentals and the measured characteristics of a state-of-the-art cryocooler design.

## ACKNOWLEDGEMENT

The work described in this paper was carried out by the Jet Propulsion Laboratory, California Institute of Technology, under a contract with the National Aeronautics and Space Administration. Particular credit is due E. Jetter who reduced much of the data to the graphs presented herein, and to S. Leland, who manufactured and assembled many of the test setups. The collaborative support of B. Jones of British Aerospace and the financial support of JPL's Pos-AIRS instrument are graciously acknowledged.

## REFERENCES

1. Ross, R. G., Jr., "JPL Cryocooler Development and Test Program Overview", 7th International Cryocooler Conference, Santa Fe, NM, November 17-19, 1992.
2. Ross, R. G., Jr., Johnson, D.L. and Sugimura, R. S., "Characterization of Miniature Stirling-cycle Cryocoolers for Space Application," Proceeding of the 6th International Cryocooler Conference, Plymouth, MA, DTRC-91 /002, David Taylor Research Center (1991), p. 27-38.
3. Kotsubo, V., Johnson, D.L. and Ross, R. G., Jr., "Cold-tip Off-state Conduction Loss of Miniature Stirling Cycle Cryocoolers," Adv. Cryo. Engin., Vol. 37B (1991), p. 1037-1043.
4. Ross, R. G., Jr., Johnson, D.L. and Kotsubo, V., "Vibration Characterization and Control of Miniature Stirling-cycle Cryocoolers for Space Application," Adv. Cryo. Engin., Vol. 37B (1991), p. 1019-1027.
5. Johnson, D. I., and Ross, R. G., Jr., "Electromagnetic Compatibility Characterization of a BAe Stirling-cycle Cryocooler for Space Applications," Adv. Cryo. Engin., Vol. 37B (1991), p. 1045-1053.

6. Kotsubo, V. Y., Johnson, D.L., and Ross, R. G., Jr., "Calorimetric Thermal-Vacuum Performance Characterization of the BAe 80 K Space Cryocooler", SAE Paper No. 929037, Proceeding of the 27th Intersociety Energy Conversion Engineering Conference, San Diego, California, August 3-7, 1992, P-259, Vol. 5, pp. 5.101-5.107.
7. Jones, B., "Long Life Stirling Cycle Cooler Developments for the Space Application Range of 20K to 80K", 7th International Cryocooler Conference, Santa Fe, NM, November 17-19, 1992.
8. Johnson, D.L., Men, G.R. and Ross, R. G., Jr., "Spacecraft Cooler Characterization", 7th International Cryocooler Conference, Santa Fe, NM, November 17-19, 1992.
9. Gottlieb, I. M., Electric Motors & Electronic Motor-control Techniques, Bobbs-Merrill Co., Inc., New York (1976).
10. A.H. Orłowska and G. Davey, "Measurement of Losses in a Stirling-cycle Cooler, " Cryogenics, vol. 27 (1987), p. 645.
11. Thomson, W .T., Vibration Theory and Applications, Prentice-Hall, Inc., Englewood Cliffs, N.J. (1965).
12. Ross, R. G., Jr., "Requirements for Long-life Mechanical Refrigerators for Space Applications", Cryogenics, Vol. 30, No.3, March 1990, p. 233-238.
13. Scull, S.R. and Jewell, C., "Pre-qualification-level Testing of an 80K Stirling-cycle Cooler", Proceedings of the 4th European Symposium on Space Environmental and Control Systems, Florence, Italy, Oct, 21-24, 1991, (ESA SP-324, December 1991).

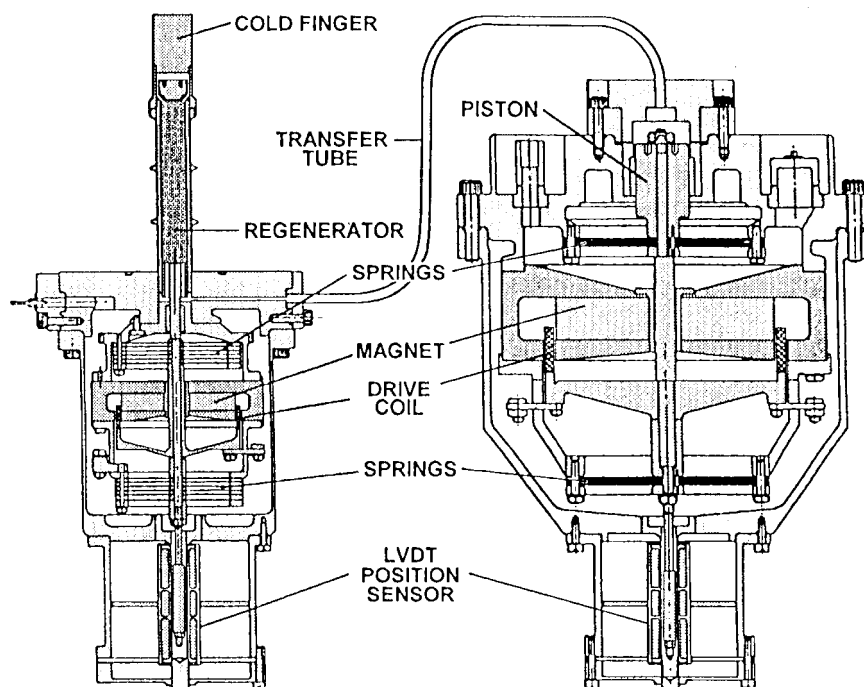


Fig. 1. Cross-section of Oxford-style Stirling-cycle cooler displaying linear drive motors and flexure-spring suspension systems.

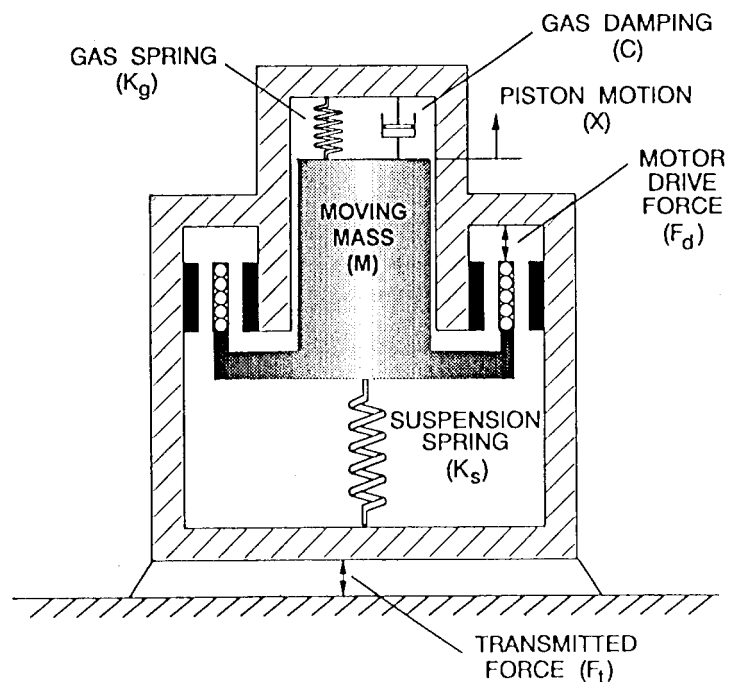


Fig. 2. Schematic representation of cryocooler compressor and displacer as single-degree-of-freedom spring-mass-damped systems.

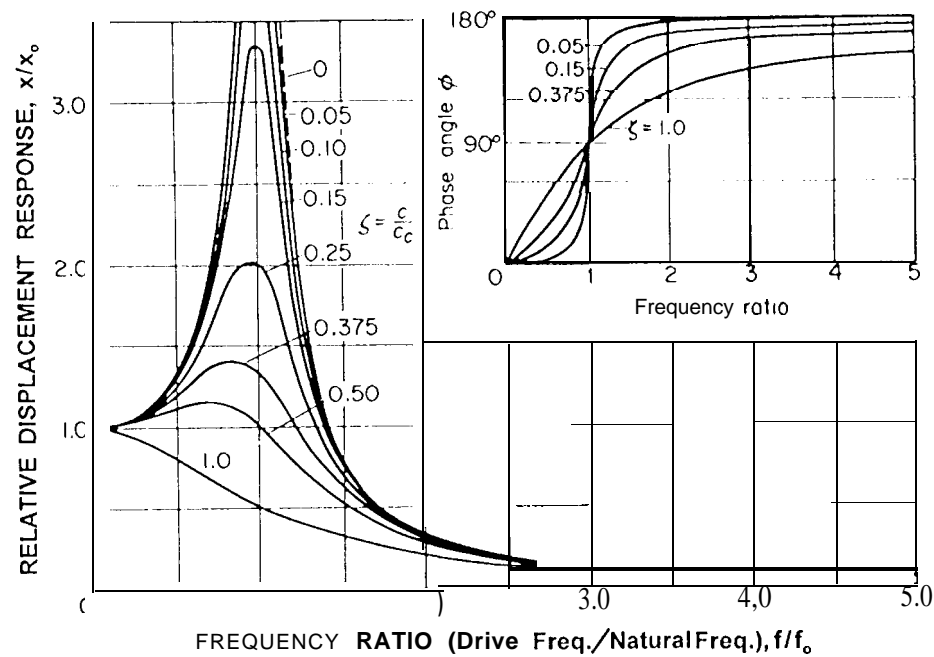


Fig. 3. Frequency response curves for 1-d.o. f. system excited by a sinusoidal force.

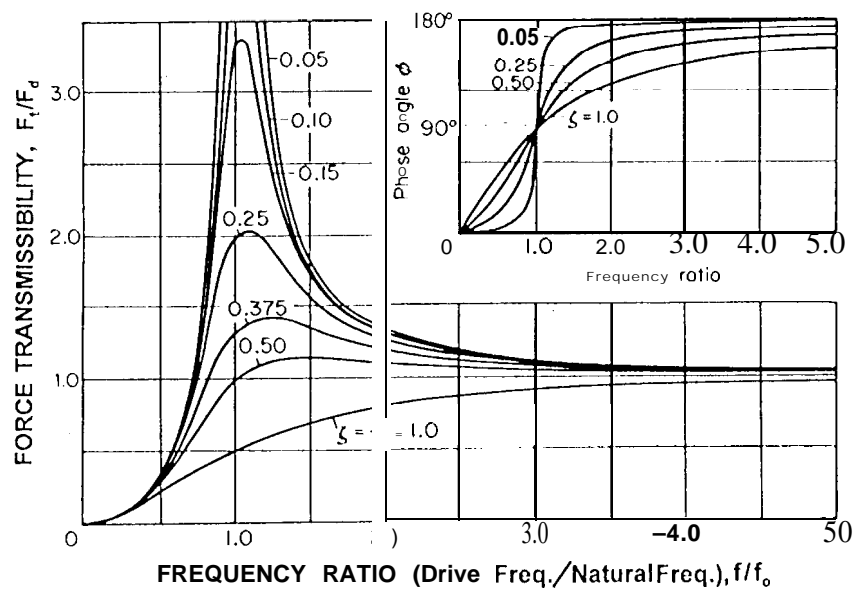


Fig. 4. Force transmissibility curves for 1-d.o. f. system excited by a sinusoidal force.

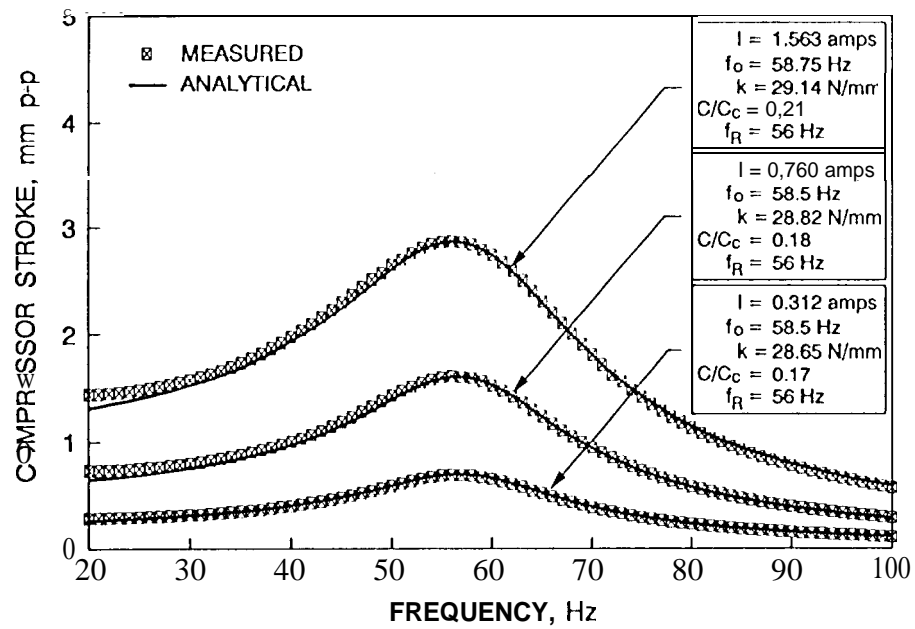


Fig. 5. Measured frequency response of BAe 55K compressor piston for constant sinusoidal drive current.

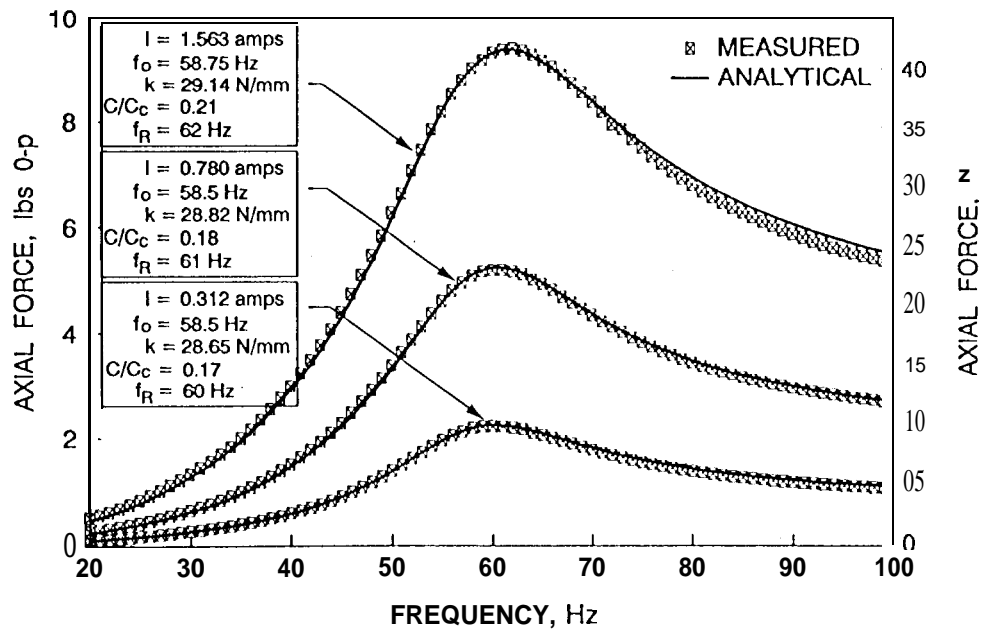


Fig. 6. Measured force transmissibility response of BAe 55K compressor for constant sinusoidal drive current.

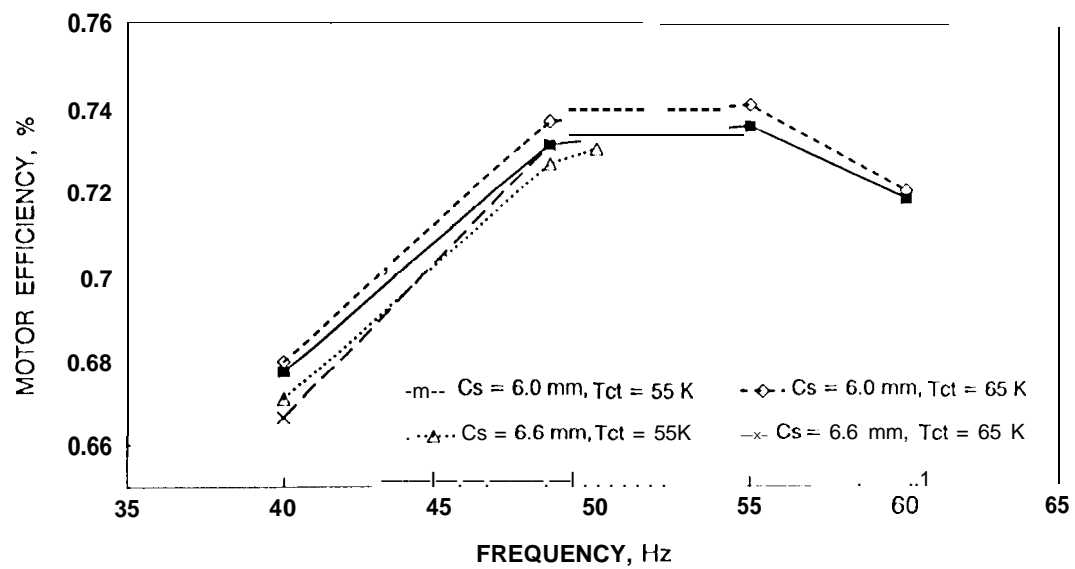


Fig. 7. Motor efficiency of the BAe 55K compressor versus drive frequency.

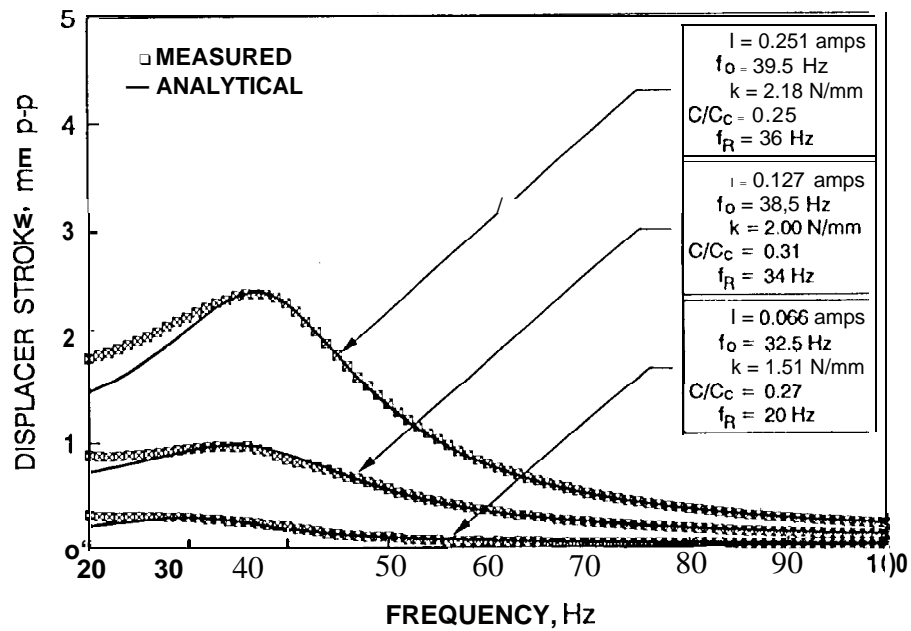


Fig. 8. Measured frequency response of BAe 55K displacer for constant sinusoidal drive current.

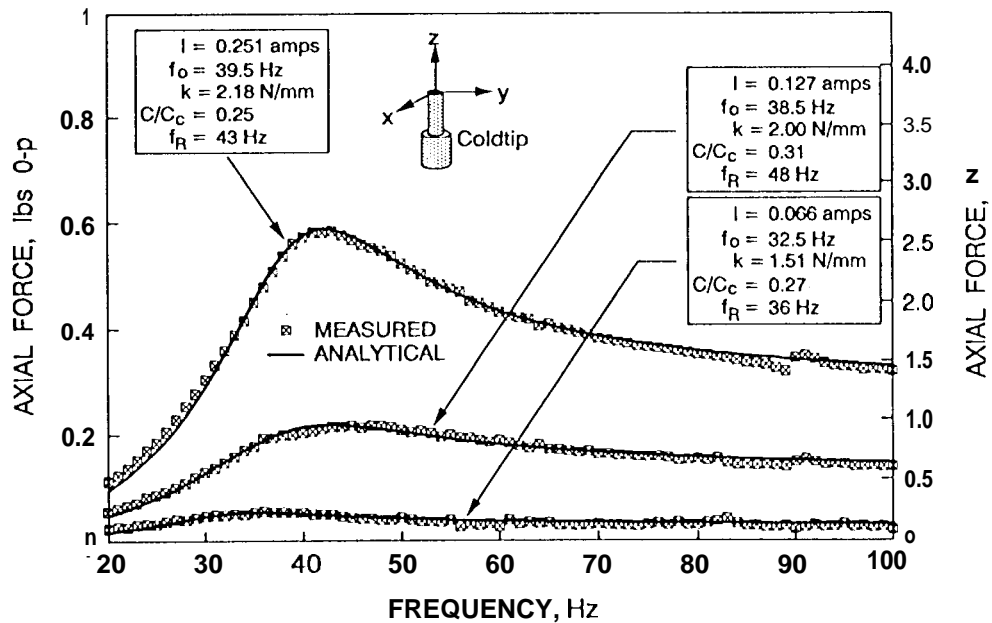


Fig. 9. Measured force transmissibility response of BAe 55K displacer for constant sinusoidal drive current.

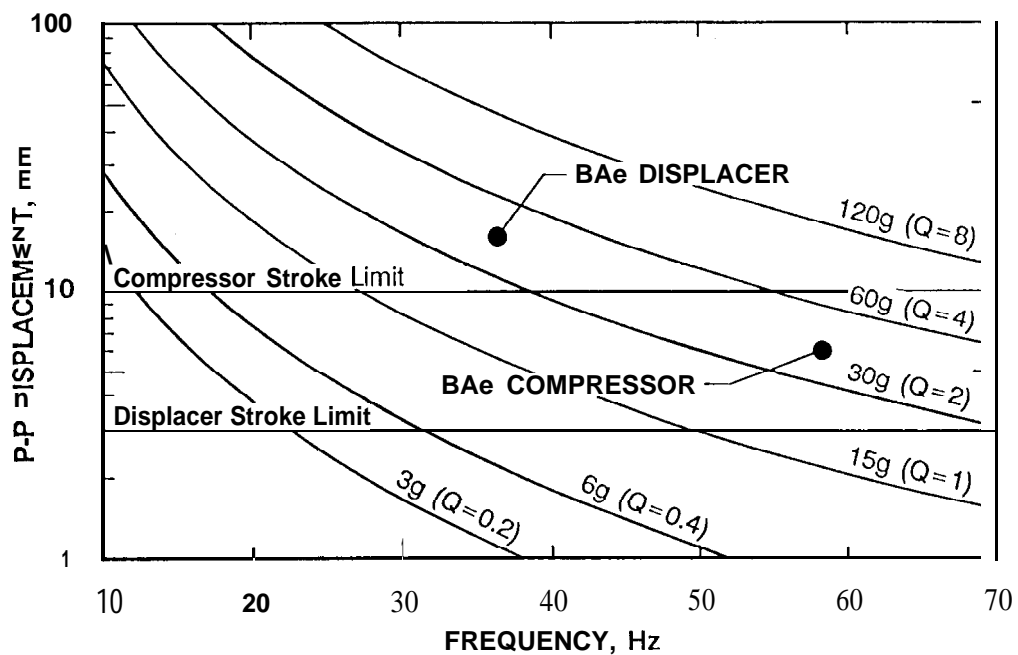


Fig. 10. Motion amplitude (p-p) at piston/displacer natural frequency ( $f_0$ ) for 15-g (o-p) sinusoidal vibration input and various amplification factors ( $Q_0$ ).

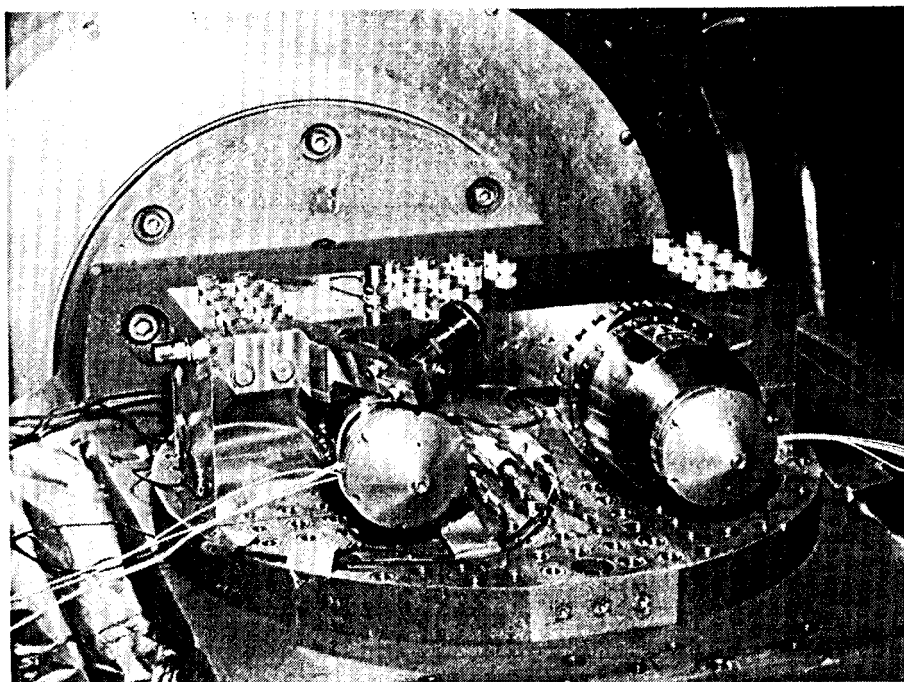


Fig. 11. BAe 55K cooler mounted in JPL launch vibration test facility.

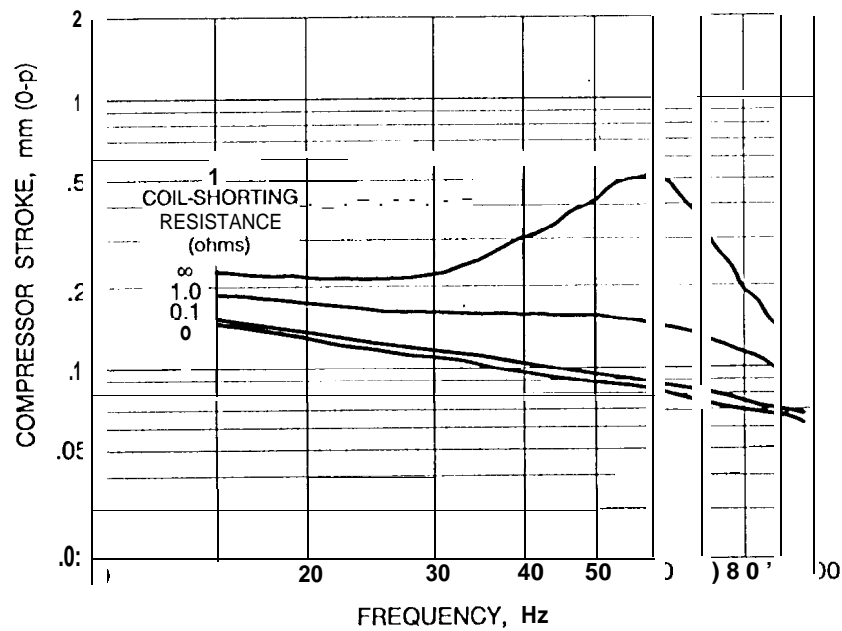


Fig. 12. Measured amplitude of compressor piston motion for BAE 55K cooler during 3-g sine sweep with various coil-shorting resistances.

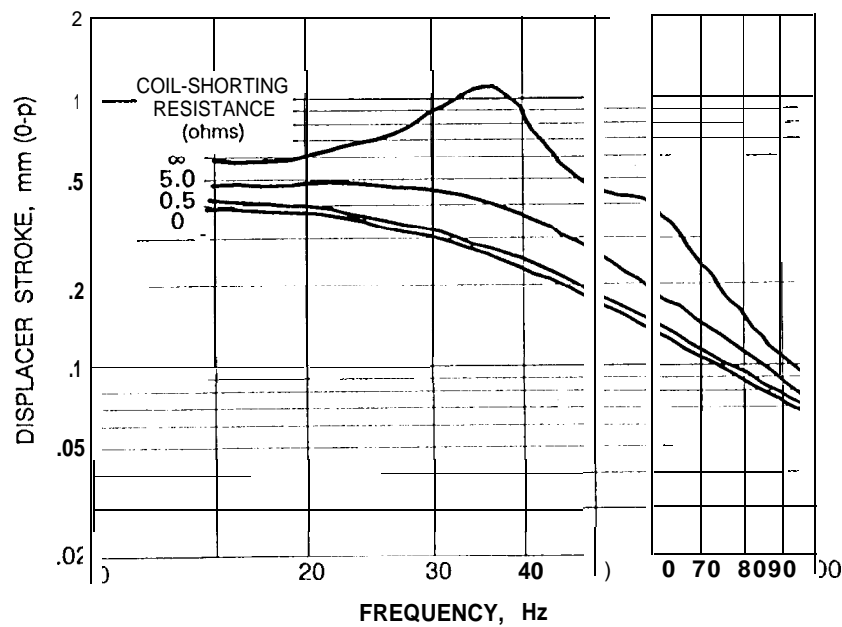


Fig. 13. Measured amplitude of displacer motion for BAE 55K cooler during 3-g sine sweep with various coil-shorting resistances.

Table 1. Summary of drive resonance parameters for BAe 55K cooler.

COMPRESSOR	COLD-TIP TEMPERATURE	
	Ambient	Cryogenic
Natural Frequency, Hz	58.5	50.2
Resonant Frequency, Hz	56.0	47.0
Motor Force Constant, N/amp	12.7	12.7
Moving Mass, g	213	213
Spring Stiffness, N/mm	28.8	21.2
Critical Damp. Coef. (CC), N-s/m	157	134
Damping Ratio, $C/C_c$	0.17-0.21	0.19-0.27
DISPLACER		
Natural Frequency, Hz	37.0	39.0
Resonant Frequency, Hz	36.0	35.0
Motor Force Constant, N/amp	7.4	7.4
Moving Mass, g	35.1	35.1
Spring Stiffness, N/mm	1.89	2.10
Critical Damp. Coef. (CC), N-s/m	16.3	17.1
Damping Ratio, $C/C_c$	0.15-0.17	0.25-0.31

Table 2. Comparison of measured and predicted response to 3-g sinusoidal acceleration input as a function of external coil-shorting resistance.

External Coil-short Resist. (ohms)	Ext. Res. plus Coil Resist. (ohms)	Open-Circuit Damping (c/cc)	Elect. Circuit Damping ( $C_e/C_c$ )	Total Damping (c/cc) + ( $C_e/C_c$ )	Gain at Natural Freq. ( $Q_{Anal}$ )	Meas. Gain at $f_o$ ( $Q_{Meas}$ )
COMPRESSOR						
$\infty$	$\infty$	0.20	0	0.20	2.50	2.36
1.0	1.88	0.17	0.55	0.72	0.69	0.64
0.1	0.98	0.17	1.05	1.22	0.41	0.40
0	0.88	0.17	1.17	1.34	0.37	0.36
DISPLACER						
$\infty$	$\infty$	0.25	0	0.25	2.00	2.04
5.0	10.6	0.25	0.32	0.57	0.88	0.80
0.5	6.1	0.25	0.55	0.80	0.63	0.52
0	5.6	0.25	0.60	0.85	0.59	0.48